Impact of Atlantic multidecadal oscillations on India/Sahel rainfall and Atlantic hurricanes

Rong Zhang[1] and Thomas L. Delworth[1]

Received 10 March 2006; revised 20 July 2006; accepted 1 August 2006; published 9 September 2006.

[1] Prominent multidecadal fluctuations of India summer rainfall, Sahel summer rainfall, and Atlantic Hurricane activity have been observed during the 20th century. Understanding their mechanism(s) will have enormous social and economic implications. We first use statistical analyses to show that these climate phenomena are coherently linked. Next, we use the GFDL CM2.1 climate model to show that the multidecadal variability in the Atlantic ocean can cause the observed multidecadal variations of India summer rainfall, Sahel summer rainfall and Atlantic Hurricane activity (as inferred from vertical wind shear changes). These results suggest that to interpret recent climate change we cannot ignore the important role of Atlantic multidecadal variability. **Citation:** Zhang, R., and T. L. Delworth (2006), Impact of Atlantic multidecadal oscillations on India/Sahel rainfall and Atlantic hurricanes, *Geophys. Res. Lett.*, *33*, L17712, doi:10.1029/2006GL026267.

1. Introduction

[2] The multidecadal fluctuations of India summer rainfall, Sahel summer rainfall, and Atlantic Hurricane activity observed in the 20th century do not appear to be related to El Nino and the Southern Oscillation (ENSO) [*Folland et al.*, 1986; *Ward*, 1998; *Goldenberg et al.*, 2001], although ENSO may modulate the inter-annual variability of these phenomena [*Ward*, 1998]. Anthropogenic climate change may contribute to the long-term decrease of 20th century Sahel rainfall [*Held et al.*, 2005], but the mechanism of the multidecadal variations is still unclear. Empirical analyses have proposed a link between an interhemispheric contrast in Atlantic sea surface temperature (SST) anomalies and Sahelian summer rainfall variations [*Folland et al.*, 1986; *Ward*, 1998]. The multidecadal variation of Atlantic hurricane activity has also been statistically linked to such Atlantic SST anomalies [*Gray*, 1990; *Landsea et al.*, 1999; *Goldenberg et al.*, 2001]. The low frequency variability in the Atlantic ocean is often called the "Atlantic Multidecadal Oscillation" (AMO), with an index defined as the area average over the entire North Atlantic of low-pass filtered (LF) annual mean SST anomalies, after removing any linear trend [*Enfield et al.*, 2001; *Sutton and Hodson*, 2005; *Knight et al.*, 2005]. The AMO is suggested to be induced by Atlantic thermohaline circulation (THC) variations and associated ocean heat transport fluctuations [*Folland et al.*, 1986; *Gray et al.*, 1997; *Delworth and Mann*, 2000; *Knight et al.*, 2005].

[3] Linkages between the AMO, Sahel summer rainfall and Atlantic Hurricane activity during the 20th century were mainly based on statistical analyses of observed data. A previous modeling study [*Vitart and Anderson*, 2001] simulated the impact of interdecadal variability in Atlantic SST on Atlantic Hurricane activity. In this study, with both statistical analyses of observed data and carefully designed experiments using the GFDL CM2.1 climate model, we show that the AMO plays a major role in forcing the 20th century multidecadal variations of India and Sahel summer rainfall, and of tropical Atlantic atmospheric circulation that is of crucial relevance for Atlantic Hurricane activity. This leads to an in-phase relationship among low frequency India and Sahel summer rainfall, and Atlantic hurricane activity. This observed variability falls within the range spanned by the individual ensemble members of our modeling experiment. In this study, we adopt the above commonly accepted definition for both the observed and modeled AMO index, as that used in many previous studies [*Enfield et al.*, 2001; *Sutton and Hodson*, 2005; *Knight et al.*, 2005]. The simple detrending applied in this definition of the AMO may not cleanly separate the THC-induced AMO signal from the anthropogenic climate change and the exact mechanism causing such defined AMO is still uncertain. However, our focus here is not on the definition or mechanism of the AMO, but on the response of the global climate system to the Atlantic multidecadal fluctuations. Here our modeling results are from just one climate model, and need to be further tested with other models. The idealized linear detrending applied to the observed variability discussed in this paper does not necessarily remove all the influence of changing external forcings. Fluctuations of the external forcings about a linear trend may have contributed to some of the observed multidecadal variability.

2. Analyses of the Impact of AMO With Observed Data

[4] We first compare the observed AMO index to time series of observed summer (June to September - JJAS) rainfall anomalies over the Sahel and west central India (Figures 1a–1c). All data were low-pass filtered (LF) with a frequency response that drops to 50% at the 10-year cutoff period to focus on the multidecadal timescale, although the unfiltered data are also shown in Figure 1. All observed data were detrended prior to analyses. There is very little linear trend in west central India summer rainfall. The Sahel summer rainfall has a decreasing trend that might be related to anthropogenic forcing [*Held et al.*, 2005], and is of the same order as the multidecadal variability. West central India is the core monsoon region, where the summer

[1]Geophysical Fluid Dynamics Laboratory, NOAA, Princeton, New Jersey, USA.

0094-8276/06/2006GL026267$05.00

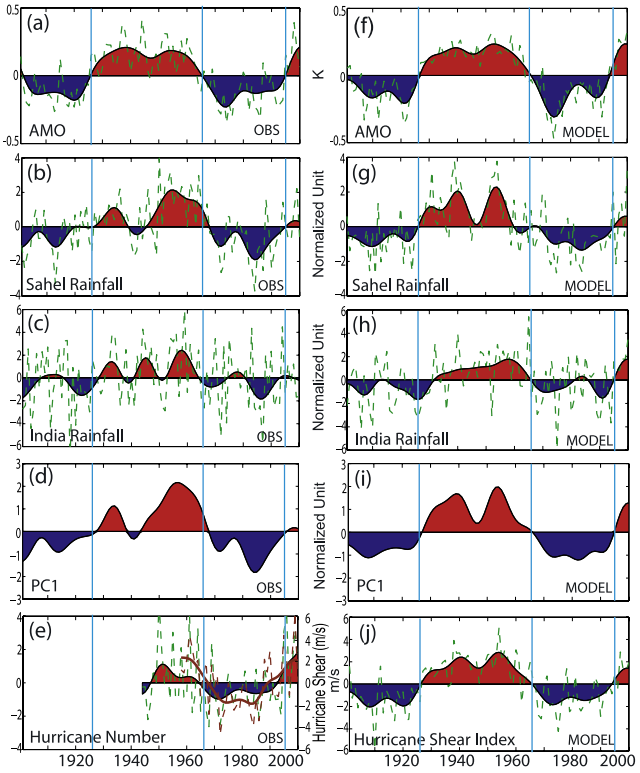

Figure 1. Observed and modeled variability. The color shading is the low-pass filtered (LF) data and the green dash line is the unfiltered data. (a) Observed AMO Index(K), derived from HADISST [*Rayner et al.*, 2003]. (b) Observed JJAS Sahel rainfall anomalies (averaged over 20°W-40°E, 10–20°N). All observed rainfall data is from Climate Research Unit (CRU), University of East Anglia, United Kingdom (CRU-TS_2.1). (c) Observed JJAS west central India rainfall anomalies (averaged over 65–80°E, 15–25°N). (d) Observed time series of the dominant pattern (PC 1) of LF JJAS rainfall anomalies. (e) Observed anomalous Atlantic major Hurricane number (axis on the left, original data from the Atlantic basin hurricane database- HURDAT, with no bias-type corrections from 1944–1969 as recently recommended by *Landsea* [2005], there is no reliable data before 1944), and observed Hurricane Shear Index (1958–2000), derived from ERA-40 [*Simmons and Gibson*, 2000] (m/s, brown solid line for LF data, brown dash line for unfiltered data, axis on the right). (f) Modeled AMO Index(K). (g) Modeled JJAS Sahel rainfall anomalies. (h) Modeled JJAS west central India rainfall anomalies. (i) Modeled PC 1 of LF JJAS rainfall anomalies. (j) Modeled Hurricane Shear Index(m/s). All LF data in this paper were filtered using the Matlab function 'filtfilt', with a Hamming window based low-pass filter and a frequency response that drops to 50% at the 10-year cutoff period. All rainfall time series are normalized by the SD of the corresponding LF data, i.e. 9.1 and 5.5 mm/month for Figures 1b and 1g; 12.5 and 7.1 mm/month for Figures 1c and 1h, 371 and 261 mm/month for Figures 1d and 1i. Light blue lines mark the phase-switch of AMO.

rainfall is highly correlated with All India Summer Rainfall [*Parthasarathy et al.*, 1994]. Over west central India, the multidecadal wet period is in phase with the positive AMO phase (warm North Atlantic) during the middle of the 20th century (~1926–1965); the dry periods are in phase with the negative AMO phase during both the early (~1901–1926) and the late 20th century (~1965–1995) (Figures 1a and 1c). The time series of west central India summer rainfall is in phase with Sahel summer rainfall (Figures 1b and 1c). The leading spatial pattern (EOF 1, from Empirical Orthogonal Function analysis, Figure 2a) of observed 20th century summer rainfall anomalies over the region covering both Africa and India also suggests an in-phase relationship between India and Sahel summer rainfall. The time series of this spatial pattern is in phase with the observed AMO index (Figures 1a and 1d).

[5] The observed AMO Index is also in phase with the observed time series of the number of major Atlantic hurricanes and the Hurricane Shear Index (Figures 1a and 1e), consistent with previous studies [*Gray*, 1990; *Landsea et al.*, 1999; *Goldenberg et al.*, 2001]. Here the Hurricane Shear Index is defined as the anomalous 200-hPa–850-hPa vertical shear of the zonal wind multiplied by −1, computed during Hurricane season, August to October-

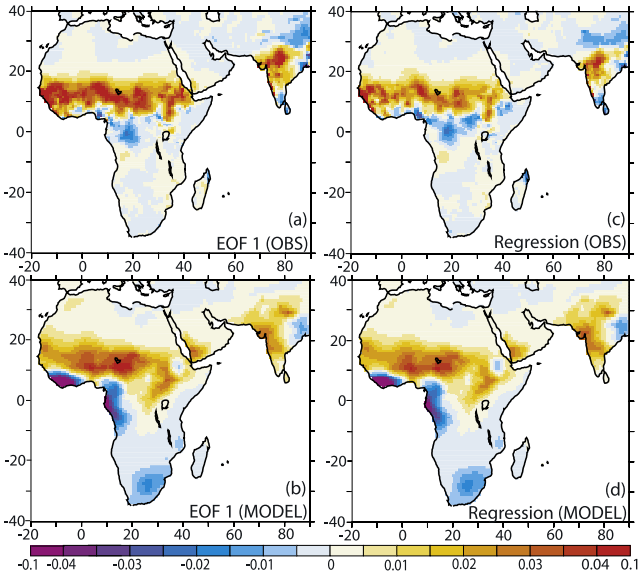

Figure 2. Leading spatial pattern of the 20th century low frequency JJAS rainfall anomalies over Africa and India. (a) EOF 1 (31%) of observed LF JJAS rainfall anomalies. (b) EOF 1 (67%) of modeled LF JJAS rainfall anomalies. (c) Regression of observed LF JJAS rainfall anomalies on observed AMO Index. (d) Regression of modeled LF JJAS rainfall anomalies on modeled AMO Index. The observed rainfall is from CRU-TS_2.1. The original regressions correspond to 1 SD of the AMO index, Figures 2a and 2c are normalized by the SD of observed time series of the dominant pattern, i.e. PC1 (371 mm/month), and Figures 2b and 2d are normalized by the SD of modeled PC1 (261 mm/month). The modeled EOF1 explains much higher percentage of variance due to ensemble average.

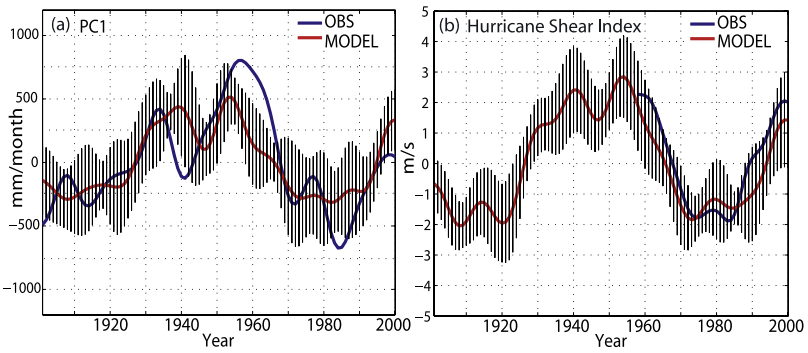

Figure 3. Observed and modeled LF variability, along with the spread over the modeled ensemble members. (a) Time series of the dominant pattern (PC 1) of LF JJAS rainfall anomalies over Africa and India (mm/month), as shown in Figures 1d and 1i but without normalization. (b) LF Hurricane Shear Index (m/s), as shown in Figures 1e and 1j. The blue solid line is observed data, the red solid line is the ensemble mean of modeling results, and the areas covered with black lines show ±1 SD (calculated from 10 ensemble members of the modeling experiment) about the ensemble mean.

ASO, and averaged over the south-central part of the main development region (MDR) of Atlantic Hurricanes (70°W-20°W, 10°N-14°N).

3. Modeling the Impact of AMO

[6] We investigate the causal link between the AMO and the above described multidecadal variability by simulating the impact of the AMO on climate with a hybrid coupled model. We employ the latest GFDL fully coupled ocean-atmosphere general circulation model (CM2.1) with levels of radiative forcing of year 1860, which produces a reasonable modern climate as observed [*Delworth et al.*, 2006]. We create a hybrid coupled model by replacing the fully dynamic ocean component of CM2.1 over the Atlantic basin (34°S-66°N) with a motionless slab ocean, which interacts with the atmosphere only through exchanges of surface heat fluxes. Ocean basins outside the Atlantic remain fully dynamic. There is a buffer zone at each of the northern and southern boundaries of the Atlantic basin, specified with the climatology from the CM2.1 control integration, to connect the slab Atlantic with other ocean basins and prevent the generation and propagation of oceanic Kelvin waves from the Atlantic to other ocean basins. We design the hybrid coupled model to assess the impact of the specified low frequency Atlantic variability through the atmospheric bridge. A climatological heat flux (qflux) diagnosed from the CM2.1 control integration, representing the effect of horizontal heat transport convergence in the ocean and heat exchange between the surface and deep ocean, is prescribed over the slab Atlantic. The control experiment of the hybrid coupled model produces a climate very similar to the control experiment of CM2.1 and to modern observations.

[7] In the perturbed experiments, in addition to the climatological qflux, we prescribe an anomalous qflux over the slab Atlantic in the hybrid coupled model to represent the AMO-like fluctuations. Observations [*Haney*, 1971] show that the ratio between surface air-sea heat flux anomaly and SST anomaly ($\partial Q/\partial SST$) over the ocean is on the order of $30 W/m^2/K$. At low frequency (multidecadal timescales), the specified qflux anomaly in the slab Atlantic should be balanced by the surface heat flux anomaly. Hence we derive the anomalous qflux pattern over the Atlantic, δQ (W/m^2), by multiplying a constant of $30 W/m^2/K$ to the observed [*Rayner et al.*, 2003] detrended Atlantic multidecadal SST difference, δSST (K), between the positive AMO phase (1941–1960) and negative AMO phase (1971–1990). We then add a small negative heat flux uniformly in the Atlantic to the anomalous qflux pattern to insure that the annual mean δQ has a zero spatial integral over the Atlantic. The qflux anomaly pattern, δQ, gives an implied increase of northward Atlantic ocean heat transport across the equator, corresponding to an increase of the Atlantic THC, and a basin-scale dipole SST anomaly (warming over the North Atlantic and cooling over the South Atlantic).

[8] We conducted a 10-member ensemble of perturbed experiments with the hybrid coupled model. Each experiment (with different initial condition from the CM2.1 control integration) is forced by the same time series of the anomalous qflux, $Q(t)$, in the Atlantic that is modulated by the observed AMO Index, $AMO(t)$, from 1901 to 2000, i.e. $Q(t) = \delta Q \times (AMO(t)/\delta AMO)$. Here $\delta AMO = 0.32K$ is the difference of the observed mean AMO value between the North Atlantic warm period (1941–1960) and cold period (1971–1990), corresponding to the anomalous qflux pattern δQ. This methodology allows us to force the model to have AMO-like fluctuations over the Atlantic. All modeled results shown are 10-member ensemble means of the perturbed experiments to reflect the impact of the imposed Atlantic variability. The ensemble approach is used to improve the signal-to-noise ratio. The modeled anomaly is defined as the difference from the 100-year average of the perturbed experiments (similar to the climatology of the control experiment). The 100-year (1901–2000) average of observed AMO Index is zero, so there is no linear trend in modeled results. All data are LF with a 10-year cutoff period.

4. Comparing Modeling Results with Analyses of Observations

[9] The simulated ensemble mean AMO index has similar phase and amplitude as the observed AMO index (Figures 1a and 1f), thereby validating the experimental design. The simulated time series of Sahel and west central India summer rainfall (Figures 1g and 1h) are in phase with the simulated

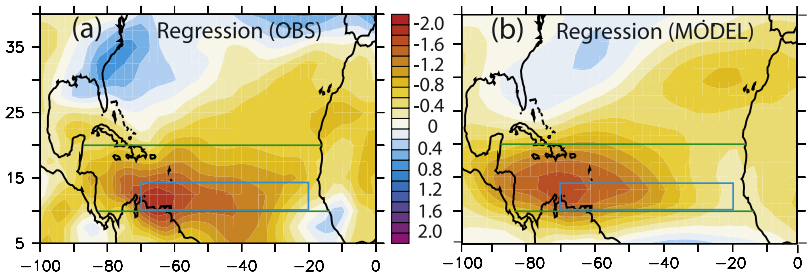

Figure 4. Regression of LF anomalous ASO vertical shear of zonal wind on the AMO Index (m/s, 1958–2000), corresponding to 1 SD of the AMO index. (a) Using ERA-40 and HADISST data. (b) Using modeled results. Green lines mark the MDR between 10°N and 20°N. The Hurricane Shear Index in Figures 1e and 1j is averaged over the blue box (70°W-20°W, 10°N-14°N, south-central part of the MDR), where the correlations between the vertical shear and major hurricanes are strongest [*Goldenberg et al.*, 2001].

AMO Index, and show similar multidecadal variations as observed (Figures 1b and 1c). The simulated dominant pattern (EOF 1) of 20th century summer rainfall over Africa and India is very similar to that observed (Figures 2a and 2b), and the associated time series shows similar multidecadal variations as observed (Figures 1d and 1i). All rainfall time series in Figure 1 are normalized by their own standard deviation (SD), and the ratio of observed to modeled SD is 1.65 (9.1 vs. 5.5 mm/month) for Sahel rainfall, 1.76 (12.5 vs. 7.1 mm/month) for west central India rainfall, and 1.42 (371 vs. 261 mm/month) for the time series of the dominant pattern (PC 1). The ensemble average usually reduces modeled amplitude of variability. The observed time series of the dominant pattern (PC 1) of LF JJAS rainfall anomalies over the region covering both Africa and India falls within the range spanned by the individual ensemble members of the modeling experiment (i.e. from the minimum to the maximum of 10 ensemble members), and generally remains within ±1 SD (calculated from 10 ensemble members) of the modeled ensemble mean (Figure 3a). The regression pattern of summer rainfall over Africa and India on the AMO Index from 1901 to 2000 (Figures 2c and 2d) is very similar to the dominant pattern (EOF 1) of summer rainfall (Figures 2a and 2b) for both observed and modeled results, suggesting that the leading pattern of multidecadal summer rainfall over Africa and India in the 20th century can be explained by the regression on the AMO Index.

[10] The simulated Hurricane Shear Index is also in phase with the simulated AMO Index over the 20th century, and has similar amplitude and phase as that observed (Figures 1f and 1j). The observed Hurricane Shear Index remains within the range spanned by the individual ensemble members of the modeling experiment, and within ±1 SD (calculated from 10 ensemble members) of the modeled ensemble mean (Figure 3b). Both observations and model results (Figure 4) show similar reductions of the vertical shear during the positive AMO phase over the tropical North Atlantic MDR, favoring the development of Atlantic Hurricanes [*Gray*, 1990; *Goldenberg et al.*, 2001]. Such reduction of vertical shear, associated warmer SST and lower sea level pressure (SLP) over the MDR, are the leading factors in the projection of the above-normal Atlantic Hurricane activity in the recent decade since 1995 when the observed AMO (Figure 1a) switched to a positive phase [*Goldenberg et al.*, 2001].

[11] In our model the positive AMO phase leads to a northward shift of the Intertropical Convergence Zone (ITCZ) and an anomalous atmospheric overturning circulation with rising motion north of the equator and descending motion south of the equator over the tropical Atlantic. Hence over the tropical North Atlantic MDR, the surface easterly trade winds are weakened and the upper level zonal winds become more westward (i.e. less westerly), resulting in a reduction of the vertical shear of the zonal wind there. Averaged over the south-central part of the MDR, the simulated change of the 200mb zonal winds is roughly four times stronger than that of the 850mb trade winds. The northward shift of the Atlantic ITCZ is associated with anomalous southwesterly surface winds over the Sahel and India, a convergence of surface moisture and thus enhanced summer monsoon rainfall over the Sahel and India. The positive AMO phase leads to warmer surface and lower SLP over Asia and Eurasia, and reduced snow cover over Tibet, which may also strengthen India summer monsoon.

[12] There are significant high correlations between the AMO and other low frequency variability. For example (Figure 5), over the 20th century, the correlation between the observed AMO and west central India summer rainfall is 0.58, significant at 95% level even with only 11 effective degrees of freedom (dof); the correlation between the observed AMO and Sahel summer rainfall is 0.71, significant at 95% level even with only 7 effective dof. Here the effective dof are derived from the decorrelation time for the correlation between variables. On the other hand, at low frequency (LF with a 10-year cutoff period), the observed detrended NINO3 index (annual mean SST anomalies

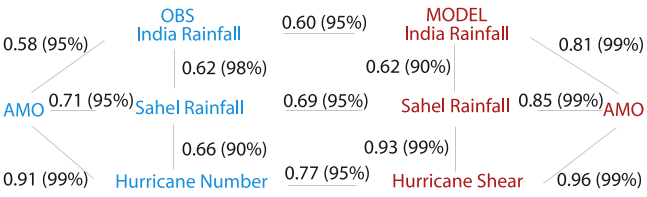

Figure 5. Correlations among LF anomalies shown in Figure 1. The correlation is shown beside the link between LF variables. The number in parentheses gives the level at which the correlation is significant with the 2-tailed Student's *t*-test, with the effective dof estimated from the decorrelation times. All correlations are over 1901–2000, except that those correlations with the observed Atlantic major Hurricane number are over 1944–2000.

averaged over 5°S-5°N and 150°W-90°W), annual mean Pacific Decadal Oscillation index, and detrended annual mean Indian Ocean SST anomalies, show non-significant low correlations (−0.17, −0.26 and −0.27 respectively) with the observed west central India summer rainfall anomaly over the 20th century. Our modeling results show significant high correlations between the modeled AMO and other modeled low frequency variability, and between modeled and observed low frequency variability, demonstrating the in-phase relationship among low frequency Sahel and India summer rainfall, and Atlantic Hurricane activity as observed (Figure 5).

5. Conclusion and Discussion

[13] Our perturbed experiments for the 20th century using the hybrid coupled model are semi-idealized experiments, which directly relate the AMO-like fluctuations to the cross-equatorial ocean heat transport anomaly. Our previous study [*Zhang and Delworth*, 2005] found that coupling to a slab ocean with specified Atlantic anomalous qflux (i.e. implied ocean heat transport anomaly induced by the THC variation) can reproduce the Atlantic ITCZ shift induced by the THC variation similar to that in a fully coupled model. Our modeling results with the hybrid coupled model suggest that the AMO plays a leading role in the 20th century multidecadal variation of India/Sahel summer rainfall and Atlantic Hurricane activity, and provide a causal link between the AMO and these variations. Our results also agree with the previous modeling study [*Vitart and Anderson*, 2001] that cooling over the tropical North Atlantic during the 1970s leads to an increase of vertical wind shear there and contributes to the reduction of Atlantic tropical storms, compared to the 1950s. A recent paleo reconstruction [*Gray et al.*, 2004] shows that the AMO has existed for the past five centuries. Although the exact mechanism causing the commonly defined AMO is still uncertain, our results indicate that the AMO-like fluctuations, which are directly associated with the ocean heat transport anomaly, have the climate impact consistent with statistical analyses of observed data.

[14] The in-phase relationship between Indian rainfall and the AMO is consistent with our previous work [*Zhang and Delworth*, 2005] showing that Indian monsoon is significantly reduced when the Atlantic THC is substantially weakened. Paleo records indicate that weakened Indian monsoons were associated with Greenland cold stadials during the last glacial period [*Altabet et al.*, 2002]. Our modeled positive AMO phase also contributes to the low summer SLP over UK region (providing a link between Sahel rainfall and UK summers), as well as the summer warming over North America and Western Europe, wetting over central America during JJA, and drought over northeast Brazil during DJF (not shown). Our modeling results suggest that if the current warm phase of the AMO persists in the coming decade, it will strengthen the summer rainfall over India and Sahel and the Atlantic Hurricane activity. Such scenario will be complicated by the influence of changing external forcings that may contribute to some of the multidecadal variability as well as the long-term trends of these phenomena. Nevertheless, our results indicate that the impact of the AMO is very important for our understanding of the future climate change.

[15] **Acknowledgments.** We thank Ants Leetmaa for the support and very helpful suggestions for this work; Isaac Held, Thomas Knutson, and Anthony Rosati for the internal review of this paper and very helpful comments. We thank Chris Landsea and an anonymous reviewer for very constructive comments on this paper. The numerical experiments were carried with the supercomputer facilities at GFDL.

References

Altabet, M. A., M. J. Higginson, and D. W. Murray (2002), The effect of millennial-scale changes in Arabian Sea denitrification on atmospheric CO2, *Nature*, *415*, 159–162.

Delworth, T. L., and M. E. Mann (2000), Observed and simulated multidecadal variability in the Northern Hemisphere, *Clim. Dyn.*, *16*, 661–676.

Delworth, T. L., et al. (2006), GFDL's CM2 global coupled climate models—Part 1: Formulation and simulation characteristics, *J. Clim.*, *19*, 643–674.

Enfield, D. B., A. M. Mestas-Nuñez, and P. J. Trimble (2001), The Atlantic multidecadal oscillation and its relation to rainfall and river flows in the continental U.S., *Geophys. Res. Lett.*, *28*, 2077–2080.

Folland, C. K., T. N. Palmer, and D. E. Parker (1986), Sahel rainfall and worldwide sea temperatures, 1901–85, *Nature*, *320*, 602–607.

Goldenberg, S. B., C. W. Landsea, A. M. Mestas-Nuñez, and W. M. Gray (2001), The recent increase in Atlantic hurricane activity: Causes and implications, *Science*, *293*, 474–479.

Gray, S. T., L. J. Graumlich, J. L. Betancourt, and G. T. Pederson (2004), A tree-ring based reconstruction of the Atlantic Multidecadal Oscillation since 1567 A.D., *Geophys. Res. Lett.*, *31*, L12205, doi:10.1029/2004GL019932.

Gray, W. M. (1990), Strong association between west African rainfall and U.S. landfall of intense hurricanes, *Science*, *249*, 1251–1256.

Gray, W. M., J. D. Sheaffer, and C. W. Landsea (1997), Climate trends associated with multidecadal variability of Atlantic hurricane activity, in *Hurricanes: Climate and Socioeconomic Impacts*, edited by H. F. Diaz and R. S. Pulwarty. pp. 15–53, Springer, New York.

Haney, R. L. (1971), Surface thermal boundary condition for ocean circulation models, *J. Phys. Oceanogr.*, *1*, 241–248.

Held, I. M., T. L. Delworth, J. Lu, K. L. Findell, and T. R. Knutson (2005), Simulation of Sahel drought in the 20th and 21st centuries, *Proc. Natl. Acad. Sci. U. S. A.*, *102*, 17,891–17,896.

Knight, J. R., R. J. Allan, C. K. Folland, M. Vellinga, and M. E. Mann (2005), A signature of persistent natural thermohaline circulation cycles in observed climate, *Geophys. Res. Lett.*, *32*, L20708, doi:10.1029/2005GL024233.

Landsea, C. W. (2005), Hurricanes and global warming, *Nature*, *438*, 11–13.

Landsea, C. W., R. A. PielkeJr., A. M. Mestas-Nuñez, and J. A. Knaff (1999), Atlantic basin hurricanes: Indices of climatic changes, *Clim. Change*, *42*, 89–129.

Parthasarathy, B., A. A. Munot, and D. R. Kothawale (1994), All-India monthly and seasonal rainfall series 1871–1993, *Theor. Appl. Climatol.*, *49*, 217–224.

Rayner, N. A., D. E. Parker, E. B. Horton, C. K. Folland, L. V. Alexander, D. P. Rowell, E. C. Kent, and A. Kaplan (2003), Global analyses of sea surface temperature, sea ice, and night marine air temperature since the late nineteenth century, *J. Geophys. Res.*, *108*(D14), 4407, doi:10.1029/2002JD002670.

Simmons, A. J., and J. K. Gibson (2000), The ERA-40 project plan, *ERA-40 Proj. Rep. Ser. 1*, 63 pp., Eur. Cent. for Med.-Range Weather Forecasts, Reading, U. K.

Sutton, R. T., and D. L. R. Hodson (2005), Atlantic Ocean forcing of North American and European summer climate, *Science*, *309*, 115–118.

Vitart, F., and J. L. Anderson (2001), Sensitivity of Atlantic tropical storm frequency to ENSO and interdecadal variability of SSTs in an ensemble of AGCM integrations, *J. Clim.*, *14*, 533–545.

Ward, M. N. (1998), Diagnosis and short-lead time prediction of summer rainfall in tropical North Africa and interannual and multi-decadal timescales, *J. Clim.*, *11*, 3167–3191.

Zhang, R., and T. L. Delworth (2005), Simulated tropical response to a substantial weakening of the Atlantic thermohaline circulation, *J. Clim.*, *18*, 1853–1860.

T. L. Delworth and R. Zhang, GFDL, NOAA, Princeton, NJ 08540, USA. (rong.zhang@noaa.gov)